Hybrid-Damped Resolved-Acceleration Control for Manipulators

Sun-Li Wu
Shir-Kuan Lin
Institute of Control Engineering
National Chiao Tung University
Hsinchu 300, Taiwan, R.O.C.

Received October 10, 1995
accepted November 4, 1996

The singularity problem of the resolved-acceleration control scheme can be solved by the damped least-squares method. This approach, however, does suffer from one serious drawback: oscillations of the end-effector when the target is outside the workspace and self-motion of the manipulator when it is at the orientation degeneracy. In this paper, we present a hybrid-damped resolved-acceleration control scheme (HDRAC), which is capable of damping both the accelerations and the velocities to overcome this drawback. The main advantage of the present approach is that the control system need not plan the path to avoid the infeasible region of the manipulator, since the controller will automatically command the end-effector to move along the boundary of the workspace with a minimum trajectory error. Thus this approach renders the resolved-acceleration control scheme a much more practical control for the industry. The stability of the proposed control scheme is also proved in this paper. Incorporated with the concept of the degenerated-direction damped least-squares method (DDDLSM), this new control scheme can also apply only to the degenerated directions, which scheme is simulated on the PUMA 560 manipulator to verify its usefulness.

分析加速度制御法の特異点問題は、減衰最小二乗法によって解決できる。しかし、この方法には、1つの大きな障害がある。それは、目標が作業空間の外にあるときのエンドエフェクタの振動と、姿勢が縮退したときのマニピュレータの自励動作である。この発表では、加速度と速度を減衰することで上記の障害を解決できる、ハイブリッド減衰分析加速度制御法（HDRAC）について説明する。この方法の主な利点は、制御システムがマニピュレータが動作不可能な領域を避けるための経路を計画する必要性がないことである。それは、コントローラが自動的に命令を送り、エンドエフェクタが最小の

CCC 0741-2223/97/080581-20

軌道誤差で作業空間の境界に沿って移動するからである。これにより、HDRACは、より実用的な工業用の制御法となる。また、この発表では、提案した制御法の安定性についても説明する。縮退進路減衰最小二乗法（DDDLSM）と組み合わせると、この新しい制御方法は、縮退進路だけに適用できる。なお、これに関してはPUMA 560マニピュレータで、その有効性を確認するシミュレーションを行っている。

1. INTRODUCTION

The resolved-acceleration control scheme[1] is a general approach for robot Cartesian control. When it is incorporated with the computed-torque method, its capability for both low- or high-speed motion control and force control is satisfactory. However, this control scheme will break down when the Jacobian matrix is singular. An effective strategy is to combine the scheme with the damped least-squares method originally proposed by Nakamura and Hanafusa[2] and Wampler.[3,4] For the sake of simplicity, this control scheme is termed *damped-acceleration resolved-acceleration control* (DARAC) in this article. However, this approach has two problems: (1) the undesirable errors in the damped least-squares solution; and (2) oscillations of the end-effector (when the target is outside the workspace) or self-motion of the manipulator (when the target is at the orientation degeneracy).

For the first problem, some researchers have proposed several variant approaches to reduce the error. One way is to damp only the small singular values of the Jacobian matrix, i.e., only the commands in the degenerated directions are sacrificed. Maciejewski *et al.*[5] used the numerical filtering method to estimate the smallest singular value and the corresponding singular vector (the degenerated direction), and then apply the damped least-squares method in the degenerated direction only. However, when the two smallest singular values cross, there is a sudden rotation of the singular vector, associated with the smallest singular value, which may cause a significant error in the estimate. So a modified method was proposed in the work of Chiaverini[6] to estimate not only the smallest singular value but also the second smallest one. Kirćanski and Borić[7,8] used the package MATHEMATICA to derive a symbolical singular value decomposition for the manipulator with a spherical wrist, such as PUMA and Stanford manipulators. This technique reduces the numerical error as well as the computation burdens, and only the small singular values are damped by the damping factor that varies with the corresponding singular value. Kirćanski *et al.*[9] implemented this technique to resolve acceleration control on a two-link manipulator. Lin and Wu[10] proposed yet another method to find the degenerated directions of the manipulator, and then applied the damped least-squares method only to them to retain the accuracy of the motion along the other directions. It is then named the degenerated-direction damped least-squares method (DDDLSM).

On the other hand, if a fixed damping factor is used, the error still remains in the damped least-squares solution when the manipulator is far away from the singular point. So several varying damping factors were adopted in the literature, such as the linear function[2,7,11–16], the second-order function[6,17], and the normal-like function.[10,18] These damping factors vary with the smallest singular value, the manipulability measure[19], or the singularity parameter.[10]

There was little discussion about the second problem mentioned above. Our experiments in the work[10] showed that oscillations of the end-effector will occur when the target is outside the workspace and self-motion of the manipulator will appear when the target is at the orientation degeneracy. Note that the workspace boundary of the redundant or nonredundant manipulator contains the singular points. We have previously proposed the damped-rate resolved-acceleration control scheme (DRRAC)[18] to damp the joint velocities, instead of the joint accelerations, to prevent the oscillations and the self-motion from occurring. By using the singular value decomposition (SVD) it is shown that the oscillations and the self-motion are due to the unnecessary nonzero joint velocities in the degenerated directions when the manipulator is at the singularity. Conceivably, the DRRAC scheme eliminates the unnecessary joint velocities in the deceleration region to overcome the disadvantage of the DARAC. However, the DRRAC raises another problem: the convergent rate of this control scheme will be slower than that of the DARAC, when the end-effector moves to a neighboring region of a singular point (i.e., the deceleration region).

This article presents the hybrid-damped resolved-acceleration control scheme (HDRAC) to overcome both the drawbacks of the DARAC and the DRRAC. When a 6 degrees-of-freedom (DOF) manipulator is at a singular configuration, it loses some DOF, assumed as k, in the task space. The controller thus has k redundant joint acceleration outputs if the resolved-acceleration control scheme is used. Fortunately, the unnecessary joint velocities and the redundant joint accelerations have the same dimensions, thus the proposed control scheme applies the redundant joint acceleration outputs to remove the unnecessary joint velocities in the deceleration region. Furthermore, the size of the deceleration region can be adjusted by a factor. It will be proved by the Lyapunov second method that the proposed control scheme is asymptotically stable and the manipulator is finally stationary whether the target is inside the workspace or not. Some simulations are undertaken on the PUMA 560 manipulator using the HDRAC incorporated with the degenerated-direction damped least-squares method[10] and a normal-like damping factor.[10,18]

The new control scheme HDRAC is significant for it is capable of making the resolved-acceleration control scheme a much more practical scheme. In the factory, the robot operators usually do not know what the singular point is, and where it is. They may ask the end-effector to bypass the outside of the workspace; oscillations or the self-motion will then occur around the singular point and will result in some damage if the DARAC is used.

This article is organized as follows: The resolved-acceleration control scheme and the damped least-squares method are reviewed in Section 2. Section 3 investigates the motion problem of the DARAC. Section 4 presents the HDRAC and the stability proof of the proposed control scheme. The degenerated-direction damped least-squares method and a normal-like damping factor are also discussed in this section. The simulations about motion near the singularity are reported in Section 5. Conclusions are drawn in the final section.

2. BACKGROUND

2.1. Resolved-Acceleration Control

The relationship between the end-effector velocities and the joint rates for the robotic manipulators can be represented as

$$\mathbf{v} \equiv \begin{bmatrix} \dot{\mathbf{r}} \\ \boldsymbol{\omega} \end{bmatrix} = \mathbf{J}\dot{\mathbf{q}} \tag{1}$$

where $\dot{\mathbf{r}}$ and $\boldsymbol{\omega}$ are the end-effector velocity and the angular velocity, respectively; $\dot{\mathbf{q}}$ is the joint rate vector; and $\mathbf{J}$ is the Jacobian matrix. Differentiating (1), we get

$$\mathbf{a} \equiv \begin{bmatrix} \ddot{\mathbf{r}} \\ \boldsymbol{\alpha} \end{bmatrix} = \mathbf{J}\ddot{\mathbf{q}} + \dot{\mathbf{J}}\dot{\mathbf{q}} \tag{2}$$

where $\ddot{\mathbf{r}}$ and $\boldsymbol{\alpha}$ are the end-effector acceleration and the angular acceleration, respectively.

It is well-known that the dynamics of a manipulator can be modelled in the form of

$$\mathbf{M}(\mathbf{q})\ddot{\mathbf{q}} + \mathbf{f}(\dot{\mathbf{q}}, \mathbf{q}) = \boldsymbol{\tau} \tag{3}$$

where $\mathbf{M}(\mathbf{q})$ is the positive definite, symmetric inertia matrix; $\mathbf{f}(\dot{\mathbf{q}}, \mathbf{q})$ is the vector comprising Coriolis, centrifugal, and gravity force, $\boldsymbol{\tau}$ is the vector of actuator force; and $\mathbf{q}$ is the vector of joint displacements. The second-order nonlinear coupled dynamic equation (3) can be linearized and decoupled by inputting the inverse dynamics

$$\boldsymbol{\tau} = \mathbf{M}(\mathbf{q})\ddot{\mathbf{q}}^* + \mathbf{f}(\dot{\mathbf{q}}, \mathbf{q}) \tag{4}$$

where $\ddot{\mathbf{q}}^*$ is the vector of the desired joint accelerations so that

$$\ddot{\mathbf{q}} = \ddot{\mathbf{q}}^* \tag{5}$$

That means, adding the inverse dynamics as a compensator in the conventional controller, the trajectory tracking in the joint coordinates is then guaranteed. This technique is called the *computed-torque* scheme.

Luh *et al.*[1] proposed the resolved-acceleration control scheme as

$$\ddot{\mathbf{q}}^* = \mathbf{J}^{-1}\mathbf{a}^* \tag{6}$$

with

$$\mathbf{a}^* = \begin{bmatrix} \ddot{\mathbf{r}}_d \\ \boldsymbol{\alpha}_d \end{bmatrix} + \mathbf{K}_D \begin{bmatrix} \dot{\mathbf{r}}_d - \dot{\mathbf{r}} \\ \boldsymbol{\omega}_d - \boldsymbol{\omega} \end{bmatrix} + \mathbf{K}_P \begin{bmatrix} \boldsymbol{\varepsilon}_r \\ \boldsymbol{\varepsilon}_e \end{bmatrix} - \dot{\mathbf{J}}\dot{\mathbf{q}} \tag{7}$$

where $\mathbf{K}_D$ and $\mathbf{K}_P$ are gain matrices; subscript d denotes the desired value; $\boldsymbol{\varepsilon}_r = \mathbf{r}_d - \mathbf{r}$ is the position error; and $\boldsymbol{\varepsilon}_e$ is the orientation error. Although the orientation error[20] can be $\theta_e\mathbf{u}_e$, $\mathbf{u}_e \tan \theta_e/2$ (Rodrigues parameters), $\mathbf{u}_e \sin \theta_e$ (the parameters of Luh *et al.*), or $\mathbf{u}_e \sin \theta_e/2$ (Euler parameters), where θ_e is the rotational angle, $\mathbf{u}_e$ is the unit vector of the rotational axis,

it is recommended to use the parameters of Luh *et al.* according to the work of Lin.[20] Unfortunately, this control scheme breaks down when $\mathbf{J}^{-1}$ does not exist, which occurs at a singular configuration.

2.2. Damped Least-Squares Method

The damped least-squares method (DLSM)[21] for the inverse problem of (1) is applied to solve the following optimization problem[2,3]

$$\min_{\dot{\mathbf{q}}} (\|\mathbf{J}\dot{\mathbf{q}} - \mathbf{v}\|^2 + \rho^2\|\dot{\mathbf{q}}\|^2) \tag{8}$$

or

$$\min_{\dot{\mathbf{q}}} \left\| \begin{bmatrix} \mathbf{J} \\ \rho\mathbf{I}_6 \end{bmatrix} \dot{\mathbf{q}} - \begin{bmatrix} \mathbf{v} \\ \mathbf{0} \end{bmatrix} \right\|^2 \tag{9}$$

where $\|\cdot\|$ denotes the Euclidean norm; ρ is a positive scalar; and $\mathbf{I}_i$ is the i-dimension identity matrix. By calculus, the solution to (9) is

$$\dot{\mathbf{q}}_\rho = \mathbf{J}_\rho^\dagger \mathbf{v} \tag{10}$$

where

$$\mathbf{J}_\rho^\dagger = (\mathbf{J}^T\mathbf{J} + \rho^2\mathbf{I}_6)^{-1}\mathbf{J}^T \tag{11}$$

which always exists for $\rho \neq 0$, since $(\mathbf{J}^T\mathbf{J} + \rho^2\mathbf{I}_6)$ is positive definite and symmetric. This solution is a compromise between the residual error, $\mathbf{J}\dot{\mathbf{q}} - \mathbf{v}$, and the magnitudes of the joint velocities, $\dot{\mathbf{q}}$, by the damping factor ρ.

The singular value decomposition (SVD) can provide insight into the singularities of the inverse Jacobian.[16] In this paper, we consider nonredundant manipulators, so $\mathbf{J}$ is a 6×6 matrix. By the theory of SVD[22], there are two orthogonal matrices $\mathbf{U} = [\mathbf{u}_1 \cdots \mathbf{u}_6]$ and $\mathbf{V} = [\mathbf{v}_1 \cdots \mathbf{v}_6]$, such that

$$\mathbf{J} = \mathbf{U}\mathbf{\Sigma}\mathbf{V}^T = \sum_{i=1}^{6} \sigma_i \mathbf{u}_i \mathbf{v}_i^T \tag{12}$$

where $\mathbf{\Sigma} = \mathrm{diag}[\sigma_1, \ldots, \sigma_6]$, σ_i are the singular values of $\mathbf{J}$, and $\sigma_1 \geq \sigma_2 \geq \cdots \geq \sigma_6 \geq 0$. The vectors $\mathbf{u}_i$ and $\mathbf{v}_i$ are the i-th left singular vector and the ith right singular vector, respectively. Substituting (12) into (11), we obtain

$$\mathbf{J}_\rho^\dagger = \mathbf{V}\mathbf{\Sigma}_\rho^\dagger\mathbf{U}^T = \sum_{i=1}^{6} \frac{\sigma_i}{\sigma_i^2 + \rho^2} \mathbf{v}_i\mathbf{u}_i^T \tag{13}$$

where $\mathbf{\Sigma}_\rho^\dagger = \mathrm{diag}[\sigma_1/(\sigma_1^2 + \rho^2), \ldots, \sigma_6/(\sigma_6^2 + \rho^2)]$.

Suppose that ρ is moderately small. When the manipulator is far from singularity (i.e., $\sigma_i \gg \rho$), then $\sigma_i/(\sigma_i^2 + \rho^2) \approx 1/\sigma_i$, which implies that $\mathbf{J}_\rho^\dagger \approx \mathbf{J}^{-1}$ [see (13)]. When the manipulator is in the neighborhood of a singular point, it can be seen from (13) that the solutions of joint velocities $\dot{\mathbf{q}}$ are not infinitely large.

$\mathbf{J}^{-1}$ in (6) is replaced by $\mathbf{J}_\rho^\dagger$ to obtain the following control scheme[9,10]

$$\ddot{\mathbf{q}}_{da}^* = \mathbf{J}_\rho^\dagger \mathbf{a}^* = \sum_{i=1}^{6} \frac{\sigma_i}{\sigma_i^2 + \rho^2} (\mathbf{u}_i^T\mathbf{a}^*)\mathbf{v}_i \tag{14}$$

We shall name the control scheme (14) the damped-acceleration resolved-acceleration control scheme (DARAC). The vector $\ddot{\mathbf{q}}_{da}^*$ in (14) is actually the solution to the optimization problem of

$$\min_{\ddot{\mathbf{q}}^*} (\|\mathbf{J}\ddot{\mathbf{q}}^* - \mathbf{a}^*\|^2 + \rho^2\|\ddot{\mathbf{q}}^*\|^2) \tag{15}$$

Note that if the ideal computed-torque control is used, the joint acceleration $\ddot{\mathbf{q}}$ is equal to $\ddot{\mathbf{q}}_{da}^*$ by (5).

3. PROBLEM STATEMENT

In this section, we state the motion problem of the DARAC in the neighborhood of the singularity and investigate the causality.

From (14), we know that any acceleration vectors in Cartesian space can be represented as a linear combination of the left singular vectors $\mathbf{u}_1, \ldots, \mathbf{u}_6$ and any joint acceleration vectors can be represented as a linear combination of the right singular vectors $\mathbf{v}_1, \ldots, \mathbf{v}_6$, since $\{\mathbf{u}_1, \ldots, \mathbf{u}_6\}$ spans a 6-dimensional space, so does $\{\mathbf{v}_1, \ldots, \mathbf{v}_6\}$. Thus, in (6), $\mathbf{a}^*$ can be represented as

$$\mathbf{a}^* = \sum_{i=1}^{6} \lambda_i \mathbf{u}_i \tag{16}$$

where $\lambda_i = \mathbf{u}_i^T\mathbf{a}^*$. Substituting (13) and (16) into (14), we get

$$\ddot{\mathbf{q}}_{da}^* = \sum_{i=1}^{6} \gamma_i \mathbf{v}_i \tag{17}$$

where $\gamma_i = \sigma_i\lambda_i/(\sigma_i^2 + \rho^2)$.

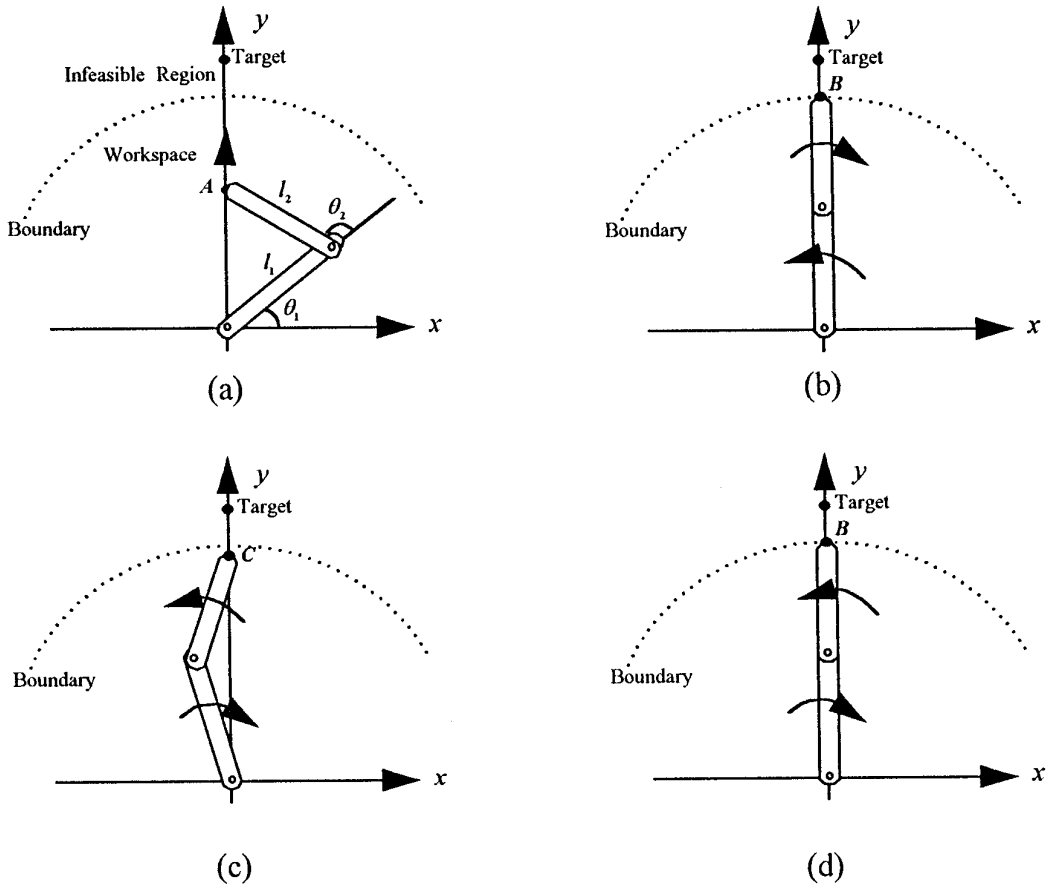

Figure 1. The motion of a two-link arm from (a), (b), (c), to (d) through the singular point B.

If the manipulator is at the singularity, we assume the rank of the Jacobian matrix is k; then $\sigma_i = 0$ and $\gamma_i = 0$ since $\gamma_i = \sigma_i\lambda_i/(\sigma_i^2 + \rho^2)$, $i = k + 1, \ldots, 6$. This implies that the components of $\ddot{\mathbf{q}}_{da}^*$ along the directions $\mathbf{v}_i$, $i = k + 1, \ldots, 6$, are zero [see (17)]. Thus, the components of $\ddot{\mathbf{q}}$ along the same directions are zero by (5). This results in that the components of $\dot{\mathbf{q}}$ along the directions $\mathbf{v}_i$, $i = k + 1, \ldots, 6$, are uncontrollable, i.e., we cannot change the values of $\dot{\mathbf{q}}$ along these directions. In general, if the target is outside the workspace or there is an infeasible region between the initial position and the target, the components of $\dot{\mathbf{q}}$ along the direction $\mathbf{v}_i$, $i = k + 1, \ldots, 6$, are nonzero when the end-effector reaches the workspace boundary containing the singular points. This occurs because, when the end-effector reaches the singular point, the acceleration commands, $\mathbf{a}^*$, in the direction $\mathbf{u}_i$ (i.e., λ_i), $i = k + 1, \ldots, 6$, are still nonzero. However, in this case, the components of $\ddot{\mathbf{q}}$ along the directions $\mathbf{v}_i$ (i.e., γ_i), $i = k + 1, \ldots, 6$, are damped to zero, implying that the components of $\dot{\mathbf{q}}$ along the directions $\mathbf{v}_i$, $i = k + 1, \ldots, 6$ stop to accelerate, yet they cannot decelerate to zero. These nonzero components of $\dot{\mathbf{q}}$ are unnecessary and will create some problems, which are stated as follows.

We shall classify degeneracy (or singularity) of a manipulator with a spherical wrist into two parts: wrist-center degeneracy and orientation degeneracy. In the nonredundant robots, whereas the wrist-center degeneracy always occurs at the workspace boundary of the manipulator, the orientation degeneracy occurs virtually any place inside the workspace. In the following discussion, we shall state the problems at these two degeneracy configurations.

The wrist-center degeneracy: We consider a two-link arm shown in Fig. 1(a). Its symbolic singular value decomposition of the Jacobian matrix[7] is

$$\mathbf{J} = \mathbf{U}\boldsymbol{\Sigma}\mathbf{V}^T = \begin{bmatrix} \text{sign}(S_2)\text{sign}(p)C_{12}u_{22} - S_{12}u_{21} & -\text{sign}(S_2)\text{sign}(p)C_{12}u_{21} - S_{12}u_{22} \\ \text{sign}(S_2)\text{sign}(p)S_{12}u_{22} + C_{12}u_{21} & -\text{sign}(S_2)\text{sign}(p)S_{12}u_{21} + C_{12}u_{22} \end{bmatrix} \times \begin{bmatrix} \sigma_1 & 0 \\ 0 & \sigma_2 \end{bmatrix} \begin{bmatrix} \text{sign}(p)v_{22} & -\text{sign}(p)v_{21} \\ v_{21} & v_{22} \end{bmatrix}^T \tag{18}$$

where $S_i = \sin\theta_i$; $C_i = \cos\theta_i$; $S_{12} = \sin(\theta_1 + \theta_2)$; $C_{12} = \cos(\theta_1 + \theta_2)$; $p = l_1 + l_2$; $u_{21} = \sigma_1\sqrt{l_2^2 - \sigma_2^2}/(l_2\sqrt{\sigma_1^2 - \sigma_2^2})$; $u_{22} = \sigma_2\sqrt{\sigma_1^2 - l_2^2}/(l_2\sqrt{\sigma_1^2 - \sigma_2^2})$; $v_{21} = \sqrt{l_2^2 - \sigma_2^2}/\sqrt{\sigma_1^2 - \sigma_2^2}$; $v_{22} = \sqrt{\sigma_1^2 - l_2^2}/\sqrt{\sigma_1^2 - \sigma_2^2}$; and the singular values are $\sigma_1 = \sqrt{h + (h^2 - 4l_1^2l_2^2S_2^2)^{1/2}}/\sqrt{2}$ and $\sigma_2 = \sqrt{h - (h^2 - 4l_1^2l_2^2S_2^2)^{1/2}}/\sqrt{2}$ with $h = l_1^2 + 2l_2^2 + 2l_1l_2\cos\theta_2$. σ_1 is never zero, while $\sigma_2 = 0$ for $\theta_2 = n\pi$, $n = 0, \pm1, \pm2, \ldots$. Note also that $u_{21} = 1$; $u_{22} = 0$; $v_{21} = l_2/\sigma_1$; and $v_{22} = l_1 \pm l_2$ when $\sigma_2 = 0$. Equations (16) and (17) are rewritten as

$$\mathbf{a}^* = \lambda_1\mathbf{u}_1 + \lambda_2\mathbf{u}_2 \tag{19}$$

$$\ddot{\mathbf{q}}_{da}^* = \frac{\sigma_1\lambda_1}{\sigma_1^2 + \rho^2}\mathbf{v}_1 + \frac{\sigma_2\lambda_2}{\sigma_2^2 + \rho^2}\mathbf{v}_2 \tag{20}$$

The tip of the two-link arm will move from a point A on the y-axis to a target point that is also on the y-axis and outside the workspace. When the tip reaches the singular point B on the boundary of the workspace [see Fig. 1(b)], $\mathbf{u}_2 = (0 \quad -1)^T$ and λ_2 is nonzero since the position error along the direction $\mathbf{u}_2$ is nonzero. However, the component of $\ddot{\mathbf{q}}_{da}^*$ along the direction $\mathbf{v}_2$ is forced to zero since $\sigma_2 = 0$ [see (20)]; the component of $\ddot{\mathbf{q}}$ along the direction $\mathbf{v}_2$ also becomes zero by (5). The component of $\dot{\mathbf{q}}$ along the direction $\mathbf{v}_2$ is nonzero, so that first link moves continuously in a counterclockwise direction and second link moves in a clockwise direction. Thus the tip is drawn from the singular point B to point C [Fig. 1(c)].

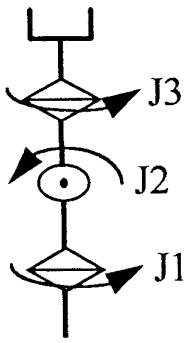

Figure 2. The spherical wrist.

As this happens, the controller will command the arm to return to the target; first link then moves in a clockwise direction and second link in a counterclockwise direction. When the tip returns to the singular point B [Fig. 1(d)], the velocities of the two links will remain nonzero, and the tip will then leave the singular point B again. Consequently, some oscillations will occur around the singular point B.

The orientation degeneracy: We consider a spherical twist which is shown in Figure 2. The singularity occurs when the first and third rotational axes are colinear, i.e., the angle of the second joint is zero. In this configuration, the component of the angular velocity of the wrist along the first rotational axis can be achieved by an infinite combination of the joint velocities of the first and third axes, since one of these two joint velocities can be vanished by the other in the opposite direction.

Suppose that we order the spherical wrist to stay in the singular configuration. When the angle of the second joint approaches zero, the joint accelerations of the first and third joints also approaches zero by the DARAC. At the same time, the joint velocities of both these joints are uncontrollable. If one of these two joint velocities is nonzero, due to the external torque or the numerical error of the controller computation, the other joint will rotate with the same period in the opposite direction. The controller cannot stop them since they are uncontrollable, so these two joints will rotate indefinitely in the singular configuration. These motions of the joints that produce no movement of the end-effector are generally referred to as self-motions.

According to the above discussions, we know that the DARAC cannot adequatelys solve the problem of robot Cartesian control near a singular point.

4. HYBRID-DAMPED CONTROL SCHEME

4.1. Control Scheme

The analysis in Section 3 implies that a good robot Cartesian control scheme should simultaneously re-

strict the velocities and the accelerations of the joints. In this paper, we consider nonredundant manipulators only. Suppose that a 6-DOF manipulator is at the singular configuration, and its rank of the Jacobian matrix is k. The manipulator will lose $6 - k$ DOF in task space. At the resolved-acceleration controller, only k DOF joint acceleration outputs are needed, but $6 - k$ DOF joint acceleration outputs are redundant, i.e., these redundant joint accelerations cannot generate the accelerations of the end-effector in any direction. On the other hand, $6 - k$ components of $\dot{\mathbf{q}}$ along the degenerated directions is unnecessary and that was stated in the last section. These two facts motivated us to propose a control scheme that uses the $6 - k$ redundant DOF joint acceleration commands to remove the $6 - k$ unnecessary components of $\dot{\mathbf{q}}$. The original optimal problem (15) will become as follows:

$$\min_{\ddot{\mathbf{q}}^*} (\|\mathbf{J}\ddot{\mathbf{q}}^* - \mathbf{a}^*\|^2 + \rho^2\|\ddot{\mathbf{q}}^* + \rho_r\dot{\mathbf{q}}\|^2) \tag{21}$$

where ρ is the damping factor that represents the weighting of the constraint $\|\ddot{\mathbf{q}}^* + \rho_r\dot{\mathbf{q}}\|$. The joint acceleration commands $\ddot{\mathbf{q}}^*$ have to minimize the additional constraint

$$\|\ddot{\mathbf{q}}^* + \rho_r\dot{\mathbf{q}}\|^2 \tag{22}$$

ρ_r is a variable dependent on the smallest singular value or singular parameter of the Jacobian matrix. When the manipulator is far away from the singular point, no joint velocity is unnecessary, thus ρ_r will be zero. If the manipulator is at a singular point, however, the unnecessary joint velocities along the degenerated directions have to be removed by the joint acceleration commands; thus ρ_r must be specified. The redundant components of the joint acceleration commands $\ddot{\mathbf{q}}^*$ will be equal to the unnecessary components of $\dot{\mathbf{q}}$ multiplied by $-\rho_r$ to minimize the constraint (22).

By calculus, we get the solution to the optimization problem (21) as

$$\begin{aligned}\ddot{\mathbf{q}}^*_{hd} &\equiv \ddot{\mathbf{q}}^*_{da} + \ddot{\mathbf{q}}^*_c \\ &= (\mathbf{J}^T\mathbf{J} + \rho^2\mathbf{I}_6)^{-1}\mathbf{J}^T\mathbf{a}^* - \rho_r\rho^2(\mathbf{J}^T\mathbf{J} + \rho^2\mathbf{I}_6)^{-1}\dot{\mathbf{q}}\end{aligned} \tag{23}$$

(23) is called the *hybrid-damped resolved-acceleration control* scheme (HDRAC). The first term on the right-hand side in (23) is equal to the solution of the DARAC. The second term, $\ddot{\mathbf{q}}^*_c$, is an additional term and is used to remove the unnecessary components of $\dot{\mathbf{q}}$, which is explained in the following.

We rewrite $\ddot{\mathbf{q}}^*_c$ in terms of the singular value decomposition of $\mathbf{J}$ as

$$\ddot{\mathbf{q}}^*_c = -\rho_r \sum_{i=1}^{6} \frac{\rho^2}{\sigma_i^2 + \rho^2} (\mathbf{v}_i^T\dot{\mathbf{q}})\mathbf{v}_i \tag{24}$$

If the manipulator is far away from any singular point, i.e., $\sigma_i \gg \rho$, $i = 1, \ldots, 6$, then $\rho^2/(\sigma_i^2 + \rho^2) \approx 0$, $i = 1, \ldots, 6$. Thus $\ddot{\mathbf{q}}^*_c$ is zero, the HDRAC is identical to the DARAC. If the manipulator is near the singular point, $\sigma_i \approx 0$, $i = k + 1, \ldots, 6$, then $\rho^2/(\sigma_i^2 + \rho^2) \approx 1$, for $i = k + 1, \ldots, 6$; hence (24) can be rewritten as

$$\ddot{\mathbf{q}}^*_c = -\rho_r \sum_{i=k+1}^{6} (\mathbf{v}_i^T\dot{\mathbf{q}})\mathbf{v}_i \tag{25}$$

In discrete-time control, we always use the back difference to approximate the derivative, so that

$$\ddot{\mathbf{q}}^*[k] = \frac{1}{\Delta t}(\dot{\mathbf{q}}^*[k] - \dot{\mathbf{q}}^*[k-1]) = \frac{1}{\Delta t}(\dot{\mathbf{q}}^*[k] - \dot{\mathbf{q}}[k]) \tag{26}$$

where Δt is the sampling time. Note that, by the assumption of the ideal computed-torque control, the measured value of $\dot{\mathbf{q}}[k]$ in this sampling interval is equal to the command $\dot{\mathbf{q}}^*[k-1]$ in the last sampling interval. For convenience the index k is dropped in the subsequent expressions; hence (26) becomes

$$\ddot{\mathbf{q}}^* = \frac{1}{\Delta t}(\dot{\mathbf{q}}^* - \dot{\mathbf{q}}) \tag{27}$$

Suppose that the unnecessary components of $\dot{\mathbf{q}}$ exist when the manipulator is at a singular point where $\sigma_i = 0$, $i = k + 1, \ldots, 6$, and we want these components of $\dot{\mathbf{q}}$ to be removed in the next sampling. That means the components of the desired joint velocities $\dot{\mathbf{q}}^*$ along $\mathbf{v}_i$, $i = k + 1, \ldots, 6$, should be zero, or $\mathbf{v}_i^T\dot{\mathbf{q}}^* = 0$, $i = k + 1, \ldots, 6$. By multiplying both sides of (27) by $\mathbf{v}_i\mathbf{v}_i^T$, $i = k + 1, \ldots, 6$, summing up the results, and setting $\mathbf{v}_i^T\dot{\mathbf{q}}^* = 0$, $i = k + 1, \ldots, 6$, we obtain

$$\sum_{i=k+1}^{6} \mathbf{v}_i\mathbf{v}_i^T\ddot{\mathbf{q}}^* = \frac{-1}{\Delta t}\sum_{i=k+1}^{6} \mathbf{v}_i\mathbf{v}_i^T\dot{\mathbf{q}} \tag{28}$$

If we choose ρ_r in (25) to be $1/\Delta t$, then $\ddot{\mathbf{q}}^*_c = \sum_{i=k+1}^{6} (\mathbf{v}_i^T\ddot{\mathbf{q}}^*)\mathbf{v}_i$ in (28), which is the additional desired joint accelerations to accomplish $\mathbf{v}_i^T\dot{\mathbf{q}}^* = 0$, $i = k + 1, \ldots, 6$. Note that $\dot{\mathbf{q}}$ in the next sampling will be equal to the desired $\dot{\mathbf{q}}^*$ if an ideal computed-torque

scheme is used. Thus, $\ddot{\mathbf{q}}_c^*$ in (25) with $\rho_r = 1/\Delta t$ will remove the unnecessary components of $\dot{\mathbf{q}}$ along $\mathbf{v}_{k+1}, \ldots, \mathbf{v}_6$ in the next sampling, while $\ddot{\mathbf{q}}_{da}^*$ in (23) make the unnecessary components of $\ddot{\mathbf{q}}$ along $\mathbf{v}_{k+1}, \ldots, \mathbf{v}_6$ zero.

For the nonredundant manipulators, the wrist-center degeneracy occurs only when the end-effector is on the workspace boundary. So the unnecessary joint velocities will be removed only in a neighborhood of the boundary. $\ddot{\mathbf{q}}_c^*$ is of no effect when the motion of the end-effector is inside the workspace. For the redundant manipulators, the singularities occur everywhere. $\ddot{\mathbf{q}}_c^*$ will remove the redundant joint velocities but it does not affect the motion of the end-effector.

From the above discussions, we choose ρ_r as

$$\rho_r = \begin{cases} \dfrac{1}{\Delta t}\left(1 - \dfrac{\sigma_{\min}}{\delta}\right) & \text{for } 0 \le \sigma_{\min} < \delta \\ 0 & \text{for } \sigma_{\min} \ge \delta \end{cases} \tag{29}$$

where $\sigma_{\min}$ is the smallest singular value or singular parameter of the Jacobian matrix. δ denotes the deceleration region. The unnecessary joint velocities will be removed when $\sigma_{\min}$ is in this region.

To make a comparison between the HDRAC and the DRRAC, we state the optimal problem of the DRRAC[18] as follows:

$$\min_{\ddot{\mathbf{q}}^*} (\|\mathbf{J}\ddot{\mathbf{q}}^* - \mathbf{a}^*\|^2 + \rho^2\|\dot{\mathbf{q}}\|^2) \tag{30}$$

and its solution is

$$\ddot{\mathbf{q}}_{dr}^* = (\mathbf{J}^T\mathbf{J} + \rho^2\mathbf{I}_6)^{-1}\mathbf{J}^T\mathbf{a}^* - \rho^2(\mathbf{J}^T\mathbf{J} + \rho^2\mathbf{I}_6)^{-1}\dot{\mathbf{q}} \tag{31}$$

There is no additional parameter ρ_r in the second term on the right-hand side of (31). The deceleration region is not adjustable, and is slightly larger than that of the HDRAC. Thus if the target is in the deceleration region, the convergent rate of this control scheme is slower than that of the DARAC when the end-effector moves into this region. By contrast, the HDRAC uses ρ_r to specify the proper deceleration region.

4.2. Stability Analysis

The following theorem shows that the HDRAC is asymptotically stable.

Theorem 1. *Let the orientation error be* $\boldsymbol{\varepsilon}_e = f(\theta_e)\mathbf{u}_e$, *where* $\mathbf{u}_e$ *and* θ_e *are, respectively, the rotational axis and angle from the current orientation to the desired one, and*

$$f(\theta_e) = \begin{cases} \theta_e, \\ \tan\dfrac{\theta_e}{2}, \\ \sin\theta_e, \\ \sin\dfrac{\theta_e}{2} \end{cases}$$

Suppose that $\rho > 0$ *and* $\rho_r > 0$ *when the manipulator is at the singular point. A sufficient condition for the global asymptotic convergence of the HDRAC in the whole workspace of the robot under the situation of* $\ddot{\mathbf{r}}_d = \dot{\mathbf{r}}_d = \mathbf{0}$ *and* $\boldsymbol{\alpha}_d = \boldsymbol{\omega}_d = \mathbf{0}$ *is that* $\mathbf{K}_D$ *is a positive-definite matrix and*

$$\mathbf{K}_P = \begin{bmatrix} k_{pr}\mathbf{I}_3 & \mathbf{0} \\ \mathbf{0} & k_{pe}\mathbf{I}_3 \end{bmatrix}$$

k_{pr} *and* k_{pe} *are positive. The equilibrium is the point of* $\dot{\mathbf{q}} = 0$.

Proof: Let the Lyapunov function be

$$V(\mathbf{q}, \dot{\mathbf{q}}) = \frac{1}{2}k_{pr}\boldsymbol{\varepsilon}_r^T\boldsymbol{\varepsilon}_r + k_{pe}\int_0^{\theta_e} f(\phi)\, d\phi + \frac{1}{2}\dot{\mathbf{q}}^T(\mathbf{J}^T\mathbf{J} + \rho^2\mathbf{I}_6)\dot{\mathbf{q}} \tag{32}$$

where

$$\boldsymbol{\varepsilon}_r = \mathbf{r}_d - \mathbf{r} \tag{33}$$

$$\int_0^{\theta_e} f(\phi)\, d\phi \equiv \begin{cases} \dfrac{\theta_e^2}{2}, & \text{for } f(\phi) = \phi, \\ -2\ln\left|\cos\dfrac{\theta_e}{2}\right|, & \text{for } f(\phi) = \tan\dfrac{\phi}{2}, \\ 1 - \cos\theta_e, & \text{for } f(\phi) = \sin\phi, \\ 2\left(1 - \cos\dfrac{\theta_e}{2}\right), & \text{for } f(\phi) = \sin\dfrac{\phi}{2}, \end{cases} \tag{34}$$

It is clear that $V(\mathbf{q}, \dot{\mathbf{q}}) \ge 0$. Evaluating $\partial V/\partial t$ along solutions of (32) yields:

$$\frac{\partial V}{\partial t} = k_{pr}\boldsymbol{\varepsilon}_r^T(\dot{\mathbf{r}}_d - \dot{\mathbf{r}}) + k_{pe}f(\theta_e)\mathbf{u}_e^T(\boldsymbol{\omega}_d - \boldsymbol{\omega}) + \dot{\mathbf{q}}^T(\mathbf{J}^T\mathbf{J} + \rho^2\mathbf{I}_6)\ddot{\mathbf{q}} + \dot{\mathbf{q}}^T\dot{\mathbf{J}}^T\mathbf{J}\dot{\mathbf{q}} \tag{35}$$

If the ideal computed-torque control is used, $\ddot{\mathbf{q}} = \ddot{\mathbf{q}}_{hd}^{*}$, then we can substitute (23) into (35) to obtain

$$\frac{\partial V}{\partial t} = k_{pr}\boldsymbol{\varepsilon}_r^T\dot{\mathbf{r}}_d + k_{pe}\boldsymbol{\varepsilon}_e^T\boldsymbol{\omega}_d + \dot{\mathbf{q}}^T\mathbf{J}^T\begin{bmatrix}\ddot{\mathbf{r}}_d\\ \boldsymbol{\alpha}_d\end{bmatrix} + \dot{\mathbf{q}}^T\mathbf{J}^T\mathbf{K}_D\left(\begin{bmatrix}\dot{\mathbf{r}}_d\\ \boldsymbol{\omega}_d\end{bmatrix} - \mathbf{J}\dot{\mathbf{q}}\right) - \rho_r\rho^2\dot{\mathbf{q}}^T\dot{\mathbf{q}} \quad (36)$$

If $\ddot{\mathbf{r}}_d = \dot{\mathbf{r}}_d = \mathbf{0}$ and $\boldsymbol{\alpha}_d = \boldsymbol{\omega}_d = \mathbf{0}$, then

$$\frac{\partial V}{\partial t} = -\dot{\mathbf{q}}^T\mathbf{J}^T\mathbf{K}_D\mathbf{J}\dot{\mathbf{q}} - \rho_r\rho^2\dot{\mathbf{q}}^T\dot{\mathbf{q}} \quad (37)$$

Since $\mathbf{K}_D$ is a positive-definite matrix, $\partial V/\partial t \leq 0$ for all $\dot{\mathbf{q}}$ and $\partial V/\partial t = 0$ only for $\dot{\mathbf{q}} = \mathbf{0}$.

Combining the above results and $V(\mathbf{q}, \dot{\mathbf{q}}) \geq 0$, we can say, by the Lyapunov theorem, that the control scheme (23) is asymptotically stable and the equilibrium solution is $\dot{\mathbf{q}} = \mathbf{0}$. ■

Consider the DARAC (14) and use the same Lyapunov function in (32) to obtain

$$\frac{\partial V}{\partial t} = -\dot{\mathbf{q}}^T\mathbf{J}^T\mathbf{K}_D\mathbf{J}\dot{\mathbf{q}} \quad (38)$$

When the manipulator is at a singular point of $\sigma_{k+1} = \cdots = \sigma_6 = 0$ and $\dot{\mathbf{q}}$ is spanned by $\mathbf{v}_i$, $i = k+1, \ldots, 6$, then $\partial V/\partial t = 0$. This implies that the equilibrium solution of the DARAC may be $\dot{\mathbf{q}} \neq 0$ when the manipulator is at the singular point. However, $\partial V/\partial t$ for the HDRAC has an additional term, $(-\rho_r\rho^2\dot{\mathbf{q}}^T\dot{\mathbf{q}})$, to ensure that $\partial V/\partial t$ is zero only when $\dot{\mathbf{q}} = 0$, i.e., the equilibrium solution of the HDRAC is $\dot{\mathbf{q}} = 0$.

The equilibrium solution $\dot{\mathbf{q}} = \mathbf{0}$ implies that all joints are stationary as $t \to \infty$ and the following facts.

1. If the target position is in the workspace or at the workspace boundary, the Lyapunov function V will decrease to zero as $t \to \infty$, i.e., the final position and orientation errors will be zero.
2. If the target position is outside the workspace, V will decrease to a constant as $t \to \infty$. This means that the end-effector will converge to a singular point that is on the boundary and the target position lies in a line along the degenerated direction. The position error cannot continue to decrease.

4.3. Degenerated-Direction Damped Least-Squares Method

We briefly review the degenerated-direction damped least-squares method[10] (DDDLSM) and extend it to the new control scheme, HDRAC.

A degenerated direction is the direction along which the component of the velocity of the end-effector cannot be generated by the joint velocities when a singular point is encountered. The DDDLSM is to apply the damped least-squares method only to the degenerated directions, so that the accuracy of the components of the velocity of the end-effector along the other directions is retained.[10] A geometrically appealing idea is to transform the representation of the Jacobian matrix to the one with respect to the frame whose axes are in alignment with the degenerated directions of the manipulator.

The only difficulty of the DDDLSM is how to find the degenerated directions of a manipulator. Fortunately, for a manipulator with a spherical wrist, the problem can be decomposed into two parts: the wrist-center degeneration and the orientation degeneration. We take the PUMA 560 robot as an illustrative example; its normal driving-axis coordinate system[23] is shown in Figure 3. Table I shows four steps to find the degenerated-direction inverse velocity relation of the PUMA 560 robot.

It is recommended[24] that the representation of the Jacobian matrix be transformed to a special form in which the linear velocity is with respect to the body-fixed frame,[3] while the angular velocity is with respect to the body-fixed frame.[5] This special form is much simpler and can be seen in Step 1 of Table I. Note that

$$\begin{bmatrix}\dot{\mathbf{r}}^{\langle 3\rangle}\\ \boldsymbol{\omega}^{\langle 5\rangle}\end{bmatrix} = \mathbf{J}^s\dot{\mathbf{q}} = \begin{bmatrix}{}^0_3\mathbf{R} & \mathbf{0}\\ \mathbf{0} & {}^0_5\mathbf{R}\end{bmatrix}\mathbf{J}\dot{\mathbf{q}} \quad (39)$$

where ${}^0_i\mathbf{R}$ is the coordinate transformation matrix from frame i to frame 0 (the base frame). Superscript $\langle i\rangle$ denotes the representation of a vector with respect to frame i. Step II is to reform the velocity relation in a form whose right upper 3×3 submatrix is zero. This is easily achieved by elementary row operations. At this moment, we can find out the singular conditions. The product of the determinants of the left-upper and the right-lower 3×3 submatrices is the determinant of the Jacobian matrix. It is apparent that

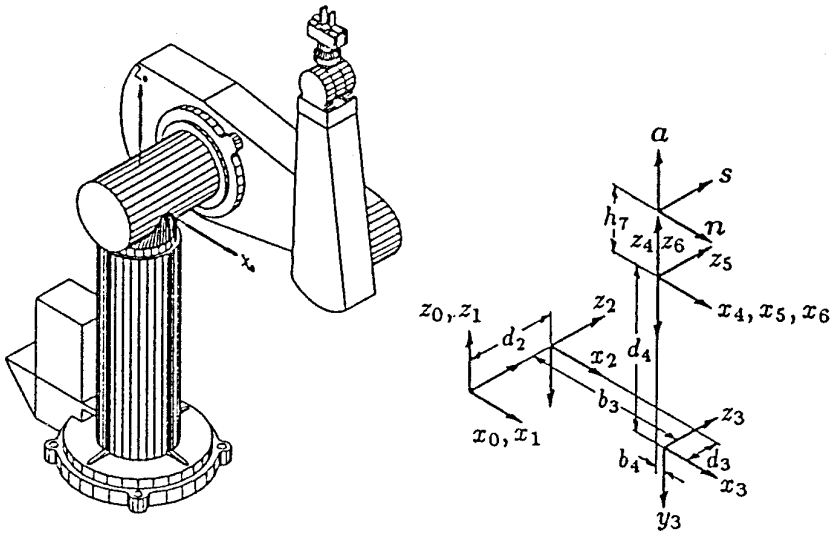

Link (Type)	Frame	θ	β	$\pm b$ (m)	$\pm d$ (m)
	E_0				
1 (R)	E_1	q_1	0°	0.	0.
2 (R)	E_2	q_2	−90°	0.	d_2
3 (R)	E_3	q_3	0°	b_3	$-d_3$
4 (R)	E_4	q_4	90°	$-b_4$	d_4
5 (R)	E_5	q_5	−90°	0.	0.
6 (R)	E_6	q_6	90°	0.	0.
	E_E	0°	0°	0.	h_7

$d_2 = 0.2435$, $b_3 = 0.4318$, $d_3 = 0.0934$
$b_4 = 0.0203$, $d_4 = 0.4331$, $h_7 = 0.14$

Figure 3. Normal driving-axis coordinate system of the PUMA 560.

the following conditions make the product of the determinants zero:

$$M \equiv b_3(C_3 d_4 + S_3 b_4) = 0 \tag{40}$$

$$N \equiv S_{23} d_4 + C_{23} b_4 + C_2 b_3 = 0 \tag{41}$$

$$S_5 \equiv \sin \theta_5 = 0 \tag{42}$$

We shall name $|M|$, $|N|$, and $|S_5|$ singularity parameters.[10] They can be used to represent the distance of the current position from the singular point. Frame 5 is a frame comprising the orientation degenerated-direction. According to geometrical analysis[10], a frame formed by the wrist-center degenerated-directions is one whose z-axis is in alignment with the z-axis of frame 3 and whose y-axis is along the direction from the origin of frame 3 to the wrist center. That means that a frame is obtained by rotating frame 3 about its z-axis by β, where $\beta = \tan^{-1}(b_4/d_4)$ is the angle between the y-axis of frame 3 and the line from the origin of frame 3 to the wrist center. We define

$$
{}^{3}_{M}\mathbf{R} \equiv \begin{bmatrix} \cos\beta & -\sin\beta & 0 \\ \sin\beta & \cos\beta & 0 \\ 0 & 0 & 1 \end{bmatrix}
= \begin{bmatrix} \dfrac{d_4}{\sqrt{b_4^2 + d_4^2}} & \dfrac{-b_4}{\sqrt{b_4^2 + d_4^2}} & 0 \\ \dfrac{b_4}{\sqrt{b_4^2 + d_4^2}} & \dfrac{d_4}{\sqrt{b_4^2 + d_4^2}} & 0 \\ 0 & 0 & 1 \end{bmatrix} \tag{43}
$$

which is the transformation matrix from the frame of the wrist-center degenerated-directions to frame

Table I. Degenerated-direction inverse-velocity relation.

Step I:

$$\mathbf{J}^s = \begin{bmatrix} -C_{23}(d_2 - d_3 + S_4S_5h_7) & S_3b_3 + C_5h_7 + d_4 & C_5h_7 + d_4 & -S_4S_5h_7 & C_4C_5h_7 & 0 \\ S_{23}(d_2 - d_3 + S_4S_5h_7) & C_3b_3 + C_4S_5h_7 - b_4 & C_4S_5h_7 - b_4 & 0 & S_5h_7 & 0 \\ J^s_{31} & 0 & 0 & C_4S_5h_7 & S_4C_5h_7 & 0 \\ -S_{23}C_4C_5 - C_{23}S_5 & S_4C_5 & S_4C_5 & -S_5 & 0 & 0 \\ S_{23}C_4S_5 - C_{23}C_5 & -S_4S_5 & -S_4S_5 & -C_5 & 0 & -1 \\ S_{23}S_4 & C_4 & C_4 & 0 & 1 & 0 \end{bmatrix}$$

$$J^s_{31} = C_{23}(C_4S_5h_7 - b_4) + S_{23}(C_5h_7 + d_4) + C_2b_3$$

Step II:

$$\dot{\mathbf{r}}^{<3>} = [w_1 \;\; w_2 \;\; w_3]^T, \; \boldsymbol{\omega}^{<5>} = [w_4 \;\; w_5 \;\; w_6]^T$$

$$\begin{bmatrix} \hat{w}_1 \\ \hat{w}_2 \\ \hat{w}_3 \\ w_4 \\ w_5 \\ w_6 \end{bmatrix} = \begin{bmatrix} -C_{23}(d_2 - d_3) & d_4 + S_3b_3 & d_4 & 0 & 0 & 0 \\ S_{23}(d_2 - d_3) & C_3b_3 - b_4 & -b_4 & 0 & 0 & 0 \\ S_{23}d_4 - C_{23}b_4 + C_2b_3 & 0 & 0 & 0 & 0 & 0 \\ -S_{23}C_4C_5 - C_{23}S_5 & S_4C_5 & S_4C_5 & -S_5 & 0 & 0 \\ S_{23}C_4S_5 - C_{23}C_5 & -S_4S_5 & -S_4S_5 & -C_5 & 0 & -1 \\ S_{23}S_4 & C_4 & C_4 & 0 & 1 & 0 \end{bmatrix} \begin{bmatrix} \dot{q}_1 \\ \dot{q}_2 \\ \dot{q}_3 \\ \dot{q}_4 \\ \dot{q}_5 \\ \dot{q}_6 \end{bmatrix}$$

$$\hat{w}_1 \equiv w_1 - (S_4h_7)w_4 - (C_4C_5h_7)w_6$$
$$\hat{w}_2 \equiv w_2 - (S_5h_7)w_6$$
$$\hat{w}_3 \equiv w_3 + (C_4h_7)w_4 - (S_4C_5h_7)w_6$$

Step III:

$$[\bar{w}_1 \;\; \bar{w}_2 \;\; \bar{w}_3] \equiv \sqrt{b_4^2 + d_4^2}\,({}^3_M\mathbf{R})[\hat{w}_1 \;\; \hat{w}_2 \;\; \hat{w}_3]$$

$$\begin{bmatrix} \bar{w}_1 \\ \bar{w}_2 \\ \bar{w}_3 \\ w_4 \\ w_5 \\ w_6 \end{bmatrix} = \begin{bmatrix} -(d_4C_{23} + b_4S_{23})(d_2 - d_3) & b_3(S_3d_4 - C_3b_4) + b_4^2 + d_4^2 & b_4^2 + d_4^2 & 0 & 0 & 0 \\ (d_4S_{23} - b_4C_{23})(d_2 - d_3) & b_3(C_3d_4 - S_3b_4) & 0 & 0 & 0 & 0 \\ S_{23}d_4 - C_{23}b_4 + C_2b_3 & 0 & 0 & 0 & 0 & 0 \\ -S_{23}C_4C_5 - C_{23}S_5 & S_4C_5 & S_4C_5 & -S_5 & 0 & 0 \\ S_{23}C_4S_5 - C_{23}C_5 & -S_4S_5 & -S_4S_5 & -C_5 & 0 & -1 \\ S_{23}S_4 & C_4 & C_4 & 0 & 1 & 0 \end{bmatrix} \begin{bmatrix} \dot{q}_1 \\ \dot{q}_2 \\ \dot{q}_3 \\ \dot{q}_4 \\ \dot{q}_5 \\ \dot{q}_6 \end{bmatrix}$$

$$\bar{w}_1 \equiv d_4\hat{w}_1 - b_4\hat{w}_2$$
$$\bar{w}_2 \equiv b_4\hat{w}_1 + d_4\hat{w}_2$$
$$\bar{w}_3 \equiv \hat{w}_3$$

Step IV:

$$\dot{q}_1 = \tfrac{1}{N}\bar{w}_3$$
$$\dot{q}_2 = \tfrac{1}{M}[\bar{w}_2 - (d_4S_{23} - b_4C_{23})(d_2 - d_3)\dot{q}_1]$$
$$\dot{q}_3 = \tfrac{1}{b_4^2 + d_4^2}\{\bar{w}_1 + (d_4C_{23} + b_4S_{23})(d_2 - d_3)\dot{q}_1 - [b_3(S_3d_4 - C_3b_4) + b_4^2 + d_4^2]\dot{q}_2\}$$
$$\dot{q}_4 = \tfrac{1}{S_5}[-w_4 - (S_{23}C_4C_5 + C_{23}S_5)\dot{q}_1 + S_4C_5(\dot{q}_2 + \dot{q}_3)]$$
$$\dot{q}_5 = w_6 - S_{23}S_4\dot{q}_1 - C_4(\dot{q}_2 + \dot{q}_3)$$
$$\dot{q}_6 = -w_5 + (S_{23}C_4S_5 - C_{23}C_5)\dot{q}_1 - S_4S_5(\dot{q}_2 + \dot{q}_3) - C_5\dot{q}_4$$

3. In Step III, the velocity relation is expressed with respect to these two degenerated frames. Step IV shows a direct way without any matrix inverse to solve the inverse velocity problem.

To apply the HDRAC only to the degenerated directions, (23) is rewritten as

$$\ddot{\mathbf{q}}^*_{hd} = (\mathbf{J}^T\mathbf{J} + \rho^2\mathbf{I}_6)^{-1}\mathbf{J}^T(\mathbf{a}^* + \rho_r\mathbf{v}) - \rho_r\dot{\mathbf{q}} \tag{44}$$

To apply the result in Table I to (44), we replace the vector $[\dot{\mathbf{r}}^{(3)^T}\ \boldsymbol{\omega}^{(5)^T}]^T$ in (39) with

$$\overline{\mathbf{a}}^* = \begin{bmatrix} {}^0_3\mathbf{R} & \mathbf{0} \\ \mathbf{0} & {}^0_5\mathbf{R} \end{bmatrix} (\mathbf{a}^* + \rho_r\mathbf{v}) \tag{45}$$

The joint acceleration commands of the HDRAC are then as

$$(\ddot{\mathbf{q}}^*_{hd})_i = \xi_i - \rho_r\dot{q}_i, \quad i = 1, \ldots, 6 \tag{46}$$

where $(\ddot{\mathbf{q}}^*_{hd})_i$ denotes the i-th component of vector $\ddot{\mathbf{q}}^*_{dr}$, and

$$\xi_1 = \frac{N}{N^2 + \rho_N^2}\overline{w}_3 \tag{47}$$

$$\xi_2 = \frac{M}{M^2 + \rho_M^2}(\overline{w}_2 - (d_4S_{23} - b_4C_{23})(d_2 - d_3)\xi_1) \tag{48}$$

$$\xi_3 = \frac{1}{b_4^2 + d_4^2}(\overline{w}_1 + (d_4C_{23} + b_4S_{23})(d_2 - d_3)\xi_1 - (b_3(S_3d_4 - C_3b_4) + b_4^2 + d_4^2)\xi_2) \tag{49}$$

$$\xi_4 = \frac{S_5}{S_5^2 + \rho_{S_5}^2}(-\omega_4 - (S_{23}C_4C_5 + C_{23}S_5)\xi_1 + S_4C_5(\xi_2 + \xi_3)) \tag{50}$$

$$\xi_5 = w_6 - S_{23}S_4\xi_1 - C_4(\xi_2 + \xi_3) \tag{51}$$

$$\xi_6 = -w_5 + (S_{23}C_4S_5 - C_{23}C_5)\xi_1 - S_4S_5(\xi_2 + \xi_3) - C_5\xi_4 \tag{52}$$

in which ρ_N, ρ_M, and ρ_{S_5} are the damping factors, and they vary with the values of N, M, and S_5, respectively. We use ρ_r as in (29) and replace $\sigma_{\min}$ in (29) by $\min(|M|, |N|, |S_5|)$.

4.4. Selection of the Damping Factor

In the DARAC and the HDRAC, ρ is used to damp the joint accelerations when the manipulator is in the neighborhood of the singularity, so that the joint accelerations are feasible for the manipulator. To improve the accuracy of the solution to these two control schemes, some varying damping factors have been adopted. In general, the linear function[2,7,11–16] is used in the form of

$$\rho = \begin{cases} \rho_{\max}\left(1 - \dfrac{\sigma}{\varepsilon}\right) & \text{for } 0 \le \sigma < \varepsilon \\ 0 & \text{for } \sigma \ge \varepsilon \end{cases} \tag{53}$$

or the second-order function[6,17] is used in the form of

$$\rho = \begin{cases} \rho_{\max}\sqrt{\left(1 - \left(\dfrac{\sigma}{\varepsilon}\right)^2\right)} & \text{for } 0 \le \sigma < \varepsilon \\ 0 & \text{for } \sigma \ge \varepsilon \end{cases} \tag{54}$$

where $\rho_{\max}$ is the maximum value of the damping factor, and is used to bound the norm of $\ddot{\mathbf{q}}^*_{da}$ when the manipulator is in the neighborhood of the singular point. σ is the smallest singular value, singular parameter, or the manipulability measure. ε defines the size of the singular region; outside this region, $\ddot{\mathbf{q}}^*_{da}$ do not have the error produced by the damping factor, while inside the region a varying damping factor is used to obtain the desired approximate solution.

In this paper, we recommend that the damping factor be a normal-like function[10], which is

$$\rho = \rho_{\max}e^{-\frac{1}{2\rho_{\max}^2}(\sigma - \rho_{\max})^2} \tag{55}$$

To compare (55) with other varying damping factors, we consider the solution of the one-dimensional DLSM, which is written as

$$\ddot{q}^*_{da} = \frac{\sigma}{\sigma^2 + \rho^2}a^* \tag{56}$$

We assume $a^* = 1$, and specify $|\ddot{q}^*_{da}| \le 25$. The singular region is defined $\sigma < 0.1$, i.e., $\varepsilon = 0.1$.

Substituting (55) into (56) yields that the maximum value of the solution $\ddot{q}^*_{da}$ is $1/(2\rho_{\max})$ at $\sigma = \rho_{\max}$, since all the 1st, 2nd and 3rd derivatives of (56) are zero and the 4th derivatives of (56) are less than zero when $\sigma = \rho_{\max}$. So, we can decide $\rho_{\max}$ in (55) is 0.02. At $\sigma = \varepsilon = 0.1$, the value of ρ approximates to zero. However, $\rho_{\max}$ in (53) and (54) are difficult to find, since we must solve a complex nonlinear equation.

Four damping factors, shown in Figure 4(a), are

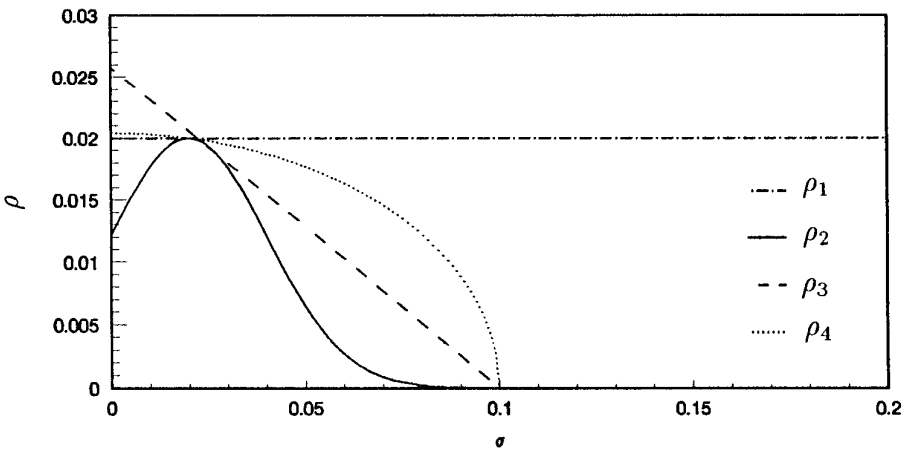

(a)

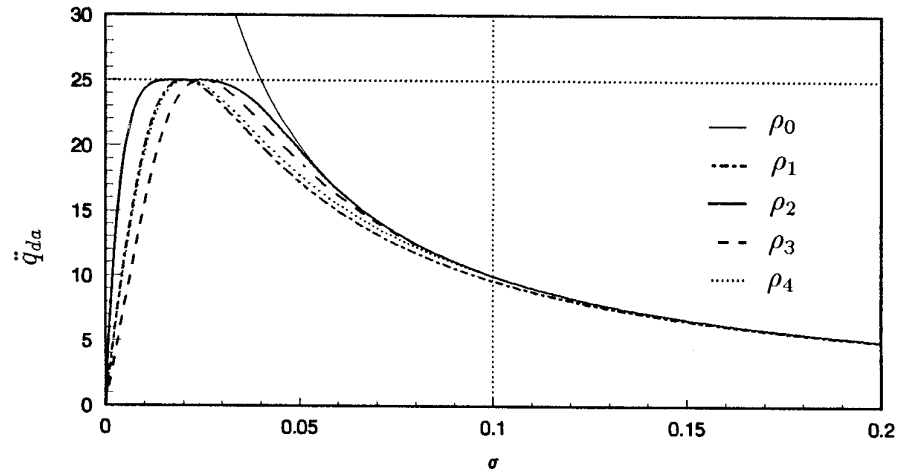

(b)

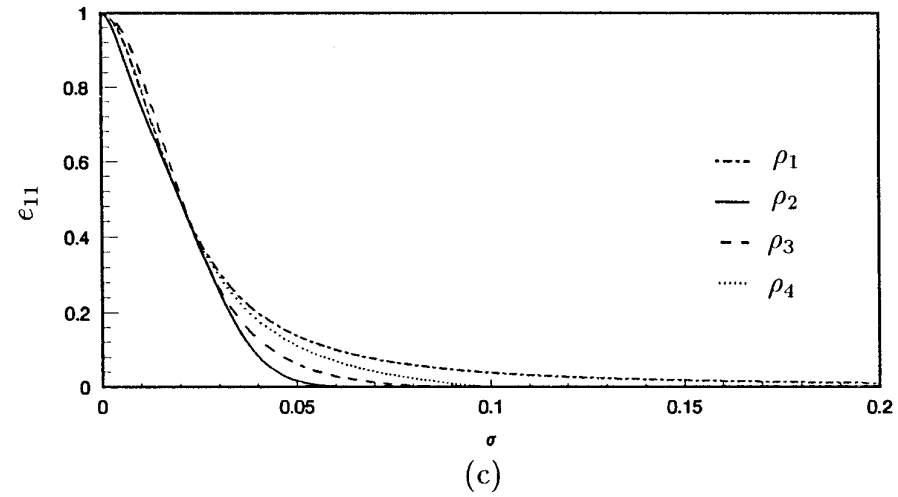

(c)

Figure 4. (a) Four damping factors, (b) the solutions of $\ddot{q}_{da}^{*}$, (c) the error function e_{11}.

substituted for (56). The fixed damping factor ρ_1 is 0.02. Other damping factors are defined as follows:

$$\rho_2 = 0.02e^{-1250(\sigma-0.02)^2} \tag{57}$$

$$\rho_3 = \begin{cases} 0.02578\left(1-\dfrac{\sigma}{0.1}\right) & \text{for } 0 \le \sigma < 0.1 \\ 0 & \text{for } \sigma \ge 0.1 \end{cases} \tag{58}$$

$$\rho_4 = \begin{cases} 0.02041\sqrt{\left[1-\left(\dfrac{\sigma}{0.1}\right)^2\right]} & \text{for } 0 \le \sigma < 0.1 \\ 0 & \text{for } \sigma \ge 0.1 \end{cases} \tag{59}$$

These damping factors, except ρ_1, satisfy the conditions: $|\ddot{q}^*_{da}| \le 25$ and $\varepsilon = 0.1$. The results are shown in Figure 4(b). The curve of ρ_0 represents the exact pseudoinverse solution, i.e., $\rho = 0$.

A good solution to (56) is close to the pseudoinverse solution and satisfies the maximum $\ddot{q}_{da}$ is 25 and $\varepsilon = 0.1$. From Figure 4(b), we know that using ρ_2 is a much better solution than using the others.

Also, an error function defined by Nakamura and Hanafusa[2] is used to make a comparison between these damping factors. This error function is defined as

$$\mathbf{e}_{11} = \mathbf{J}(\ddot{\mathbf{q}}^* - \ddot{\mathbf{q}}^*_{da}) \tag{60}$$

It denotes the end-effector acceleration error caused by the difference of the pseudoinverse solution $\ddot{\mathbf{q}}^*$ and the damped least-squares solution $\ddot{\mathbf{q}}_{da}$.

By applying (60) to (56), the error function can be rewritten as

$$e_{11} = \frac{\rho^2}{\sigma^2 + \rho^2} \tag{61}$$

The variations of the error e_{11} for the four damping factors (ρ_1, ρ_2, ρ_3, and ρ_4) are shown in Figure 4(c). From this figure, it is clear that the error produced by ρ_2 is smaller than that produced by the others.

5. SIMULATIONS

Five examples are given in this section. The simulation object is the PUMA 560 robot. The control schemes in the simulations are all applied only to the degenerated directions (see section 4.3). The performance of the HDRAC (46) is compared with that of the DARAC[10] in the first three examples. The fourth example presents a comparison of the convergent rates for using the DARAC, the DRRAC, and the HDRAC. The last example shows the effects of the four damping factors on the HDRAC. The input commands of all simulations are step commands. The controller parameters are set as $\mathbf{K}_P = 64\ \mathbf{I}_6$, $\mathbf{K}_D = 16\ \mathbf{I}_6$, and the sampling period is 3 ms.

In the first four examples, the damping factors in (47), (48), and (50) are chosen as

$$\rho_M = 0.02e^{-1250(|M|-0.02)^2} \tag{62}$$

$$\rho_N = 0.02e^{-1250(|N|-0.02)^2} \tag{63}$$

$$\rho_{S_5} = 0.01e^{-5000(|S_5|-0.01)^2} \tag{64}$$

i.e., the normal-like functions (55). The second damping factor ρ_r of the HDRAC is defined in (29) with $\delta = 0.02$.

Example 1

The first example illustrates the responses of the manipulator if there is an infeasible region between the desired position and the initial position. The initial position is (−0.1, 0.2, 0.8) and the desired position is (0.15, −0.15, 0.6), while the orientation is ignored. Figure 5 shows the projections of the response trajectories of the end-effector on the x-y plane. The result of the DARAC is in Figure 5(a). The singular circle ($N = 0$) in the figure is the boundary of the workspace, the infeasible region is inside it, and the workspace of the manipulator is outside it. When the end-effector touches the circle, it leaps away from the circle immediately. But after it has touched the singular circle three times, the end-effector then reaches the desired position. Figure 5(b) is the simulation result of the HDRAC. In this figure, the trajectory has only a small fluctuation when the end-effector first touches the singular circle; then it moves along the circle until there is no infeasible region between the position of the end-effector and the target.

To support our recommendation to apply the HDRAC only to the degenerated directions (i.e., the DDDLSM version), we repeat example one with the DLSM version of the HDRAC (i.e., all directions are damped). The end-effector trajectories are shown in Figure 6, where the dashed line denotes the result of the DLSM version and the solid line denotes that of the DDDLSM version. From this figure, we know that the response of the DDDLSM version is faster. This result clearly demonstrates the advantage of the DDDLSM version over the DLSM version. The reason

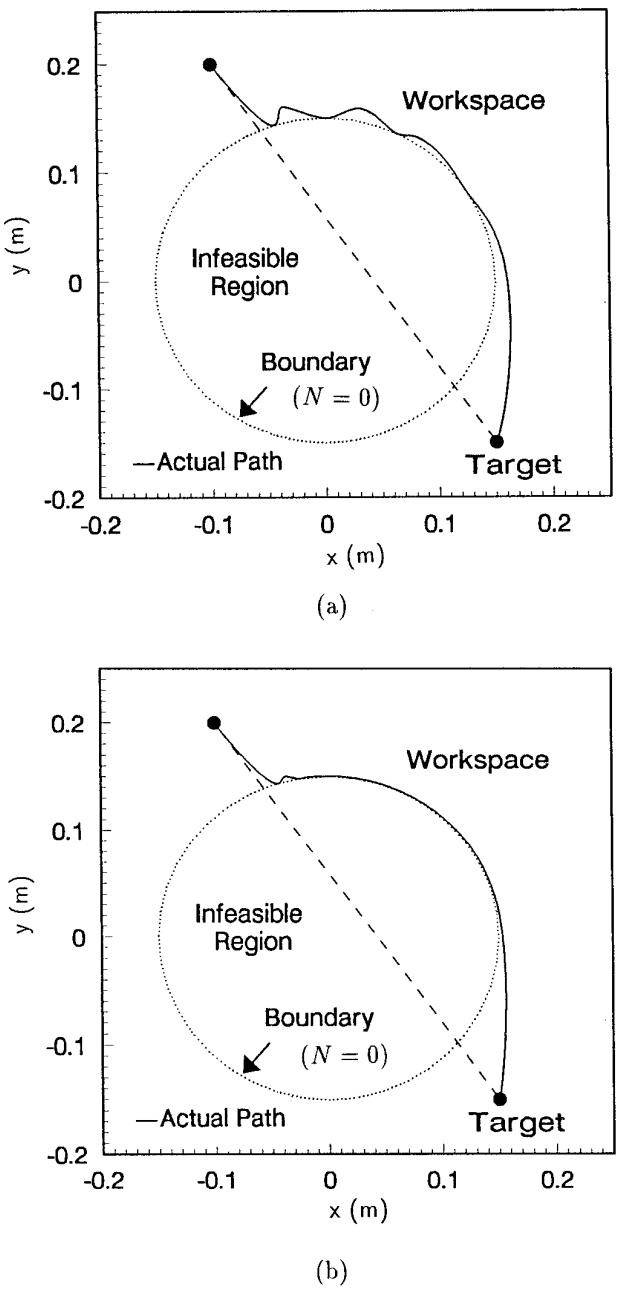

Figure 5. The trajectories for example 1: (a) with the DARAC, (b) with the HDRAC.

is that the components of the joint accelerations along the other directions rather than the degenerated ones are retained.

Example 2

In example 2, the target is outside the workspace of the manipulator. The initial position and the target are (−0.1, 0.2, 0.8) and (−0.05, 0.05, 0.8), respectively. The simulation result for the DARAC is shown in Figure 7(a). After the end-effector has touched the singular circle, oscillations occur around the workspace boundary. The result of the HDRAC in Figure 7(b), however, shows that the end-effector moves along the workspace boundary without any oscillations, after the end-effector has touched the circle. Finally, the end-effector converges to a singular point nearest to the target. Figure 7(c) presents the position errors of the two control schemes and indicates that the performance of the HDRAC is more desirable.

Example 3

Example 3 illustrates the response of the manipulator in the orientation degeneracy. The initial position and the target are, respectively, (−0.1, 0.2, 0.94) and (−0.0203, 0.1501, 1.0049), and the orientation holds unchanging towards the positive z-axis. At the target, q_5 is zero, i.e., a singular point. The joint displacements of the joints 4, 5, and 6 for the DARAC are shown in Figure 8(a). In this figure, when $q_5 = 0$, joints 4 and 6 rotate with the same speed but in the opposite directions. The reason is that the DARAC forces $\ddot{q}_4^*$ and $\ddot{q}_6^*$ to zero, but allows $\dot{q}_4$ and $\dot{q}_6$ to remain nonzero, when $q_5 = 0$. The result of the HDRAC is shown in Figure 8(b). When q_5 approaches 0, both joints then stop at the same time, which verifies the theory in section 4.2.

Example 4

When the target is in the deceleration region (including the singular point), the convergent rate of the DRRAC is slower than those of both the DARAC and the HDRAC. In example 4, we use these three control schemes to move the end-effector from (−0.1, 0.2, 0.8) to the singular point (0, 0.1501, 0.8). The results are shown in Figure 9. It can be seen from this figure that the position errors of the DARAC and the HDRAC converge to zero by 1.2 s, while the DRRAC still has about 2 mm error at 1.2 s.

Example 5

Example 5 shows the effects of the damping factors ρ_1, ρ_2, ρ_3, and ρ_4 [see (57)-(59)] on the HDRAC. The end-effector is asked to move from the singular point (0, 0.1501, 0.8) (this point is a singular point of $N = 0$) along the degenerated direction to the point

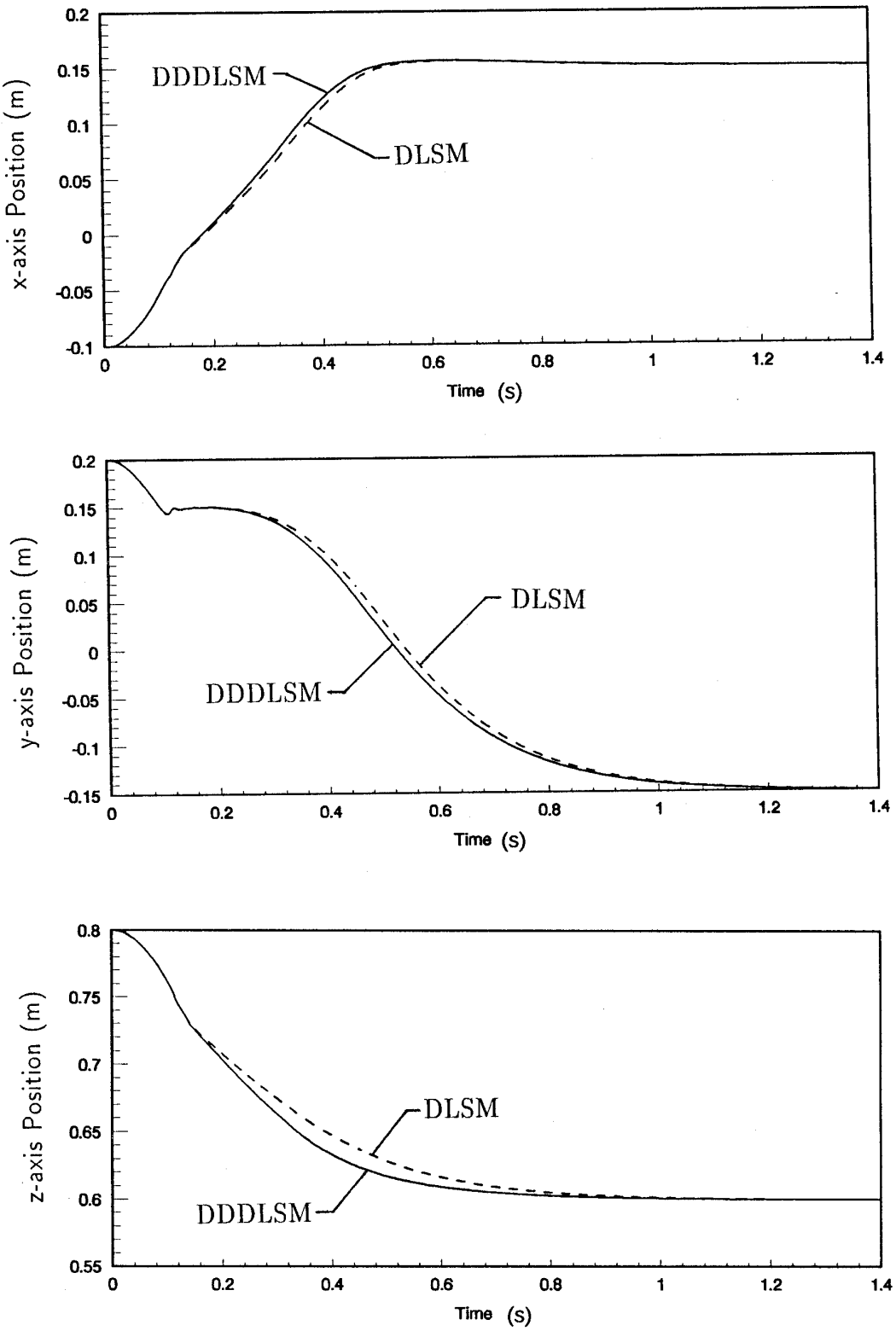

Figure 6. The trajectories for example 1 (DLSM, dashed; DDDLSM, solid).

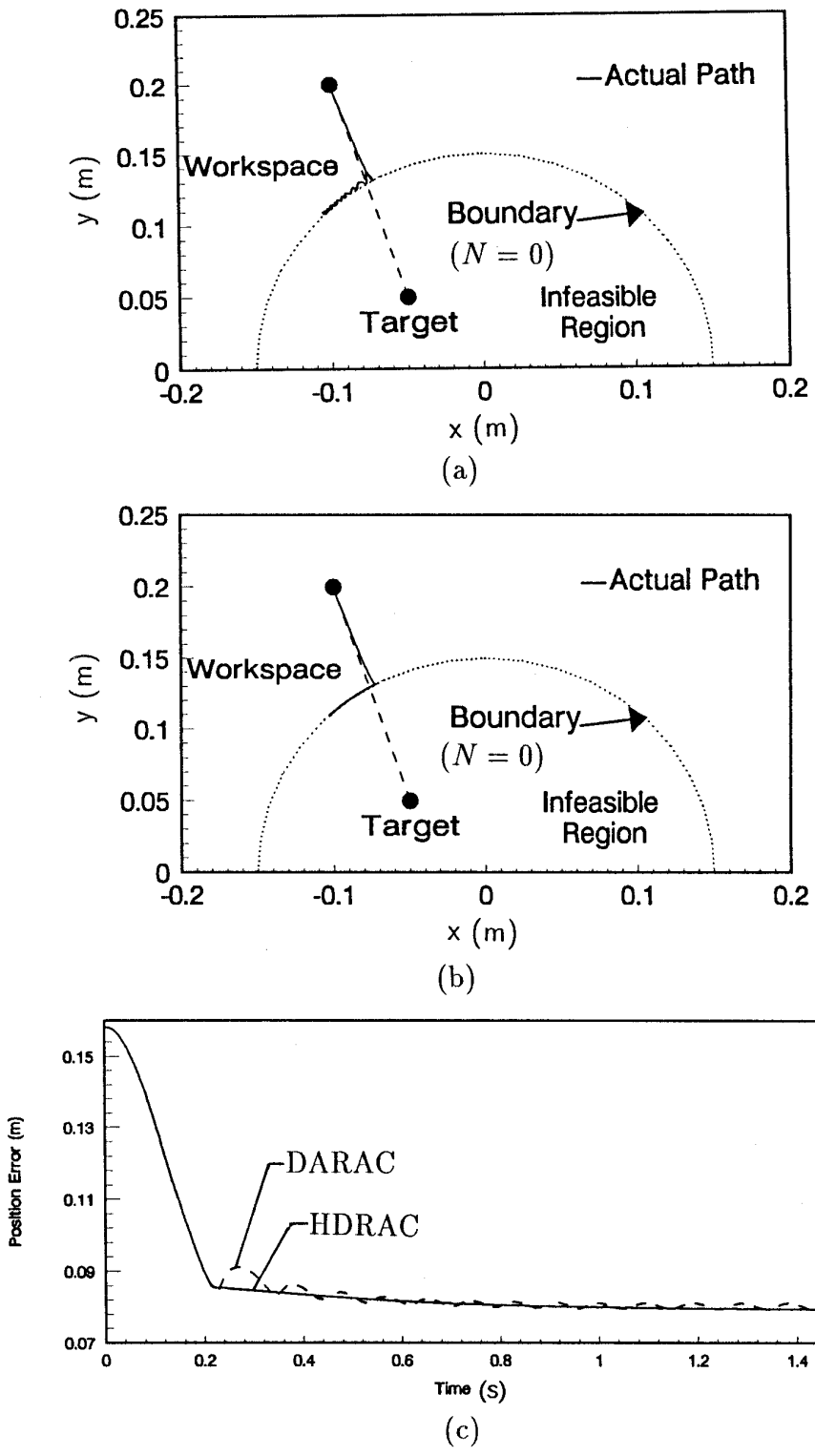

Figure 7. The trajectories projected on x-y plane for example 2: (a) with the DARAC, (b) with the HDRAC, (c) the position errors (DARAC, dashed; HDRAC, solid).

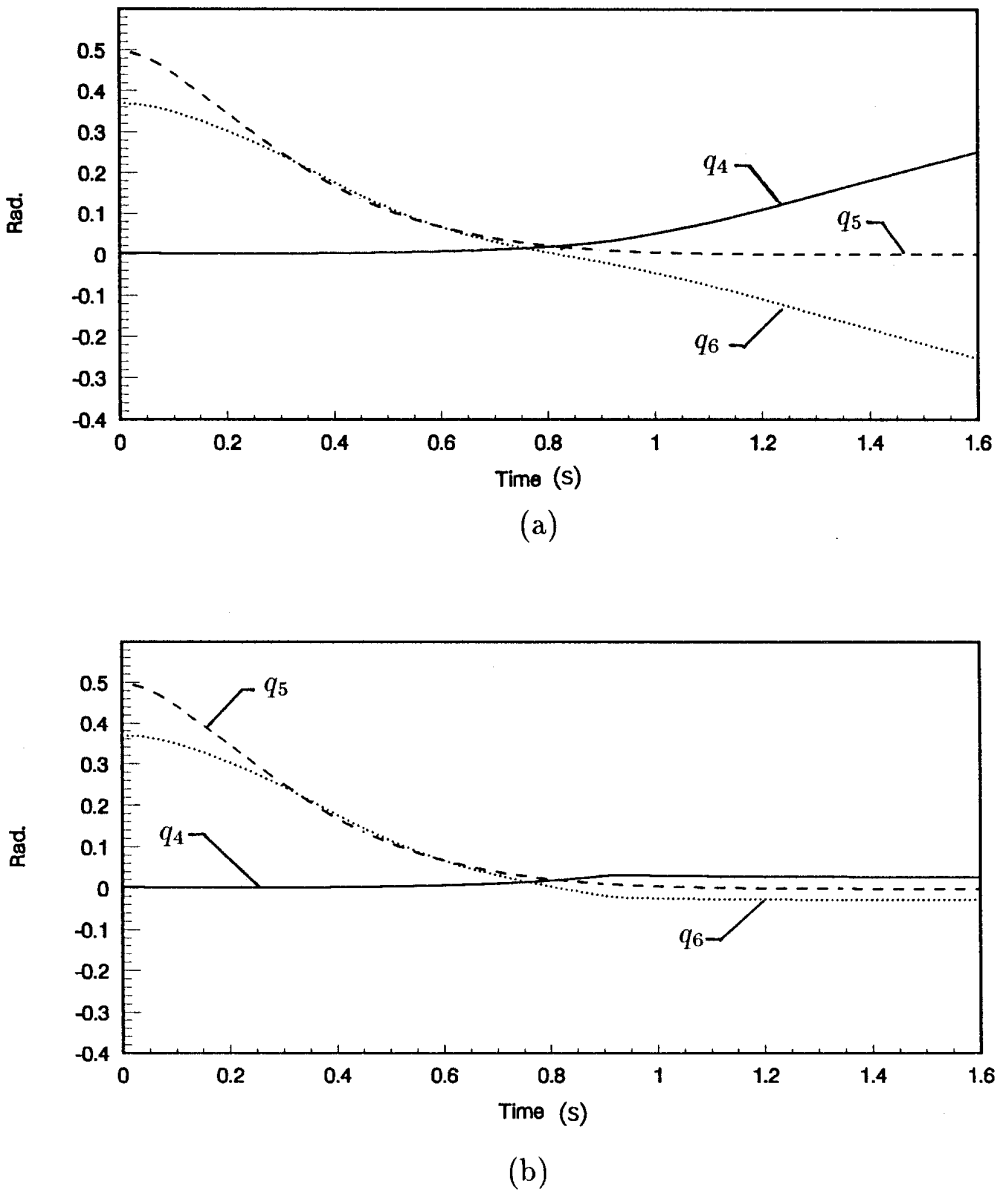

Figure 8. The time-history of q_4, q_5, and q_6 for example 3: (a) with the DARAC, (b) with the HDRAC.

(0, 0.2, 0.8). We selected a singular point as the initial position because different damping factors have different properties in the neighborhood of the singular point. Theoretically, the end-effector cannot move along the degenerated direction when it is at the singular point. However, the end-effector is not precisely at the singular point since the computations of the controller have very small numerical errors. Thus, in the simulation, the end-effector can leave the singular point along the degenerated direction, but there is a time delay in the movement from the time at which the controller accepts the command. This time delay occurs because the projection of the joint accelerations on the degenerated direction is so small that the end-effector leaves the singular point slowly. The results in Figure 10 shows the superiority of the normal-like damping factor ρ_2 to the other damping factors. These phenomena can be explained by Figure 4(b), which shows that ρ_2 has the largest joint accelerations in the neighborhood of the singular point to render the end-effector to move more quickly.

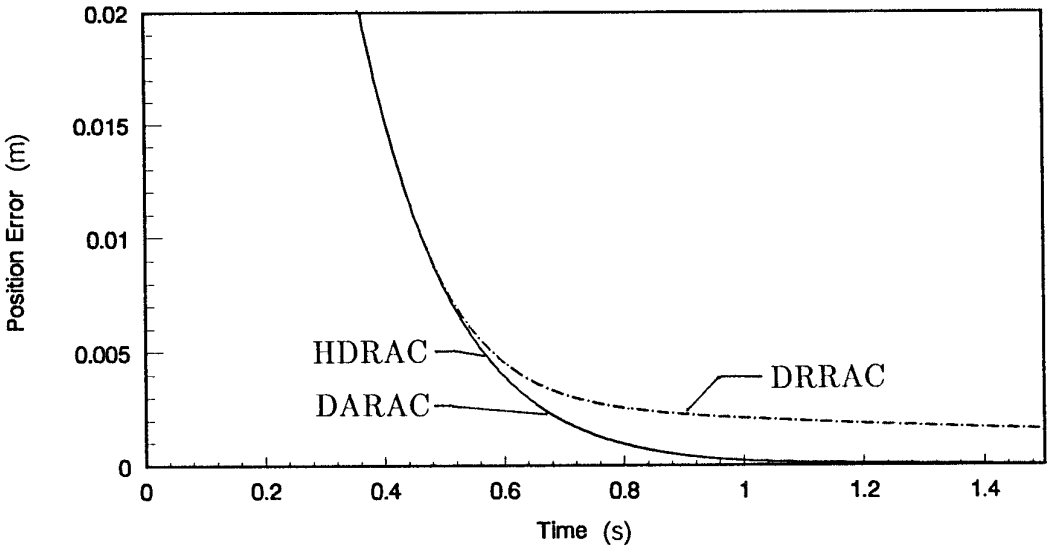

Figure 9. The position errors of the DARAC, the DRRAC, and the HDRAC for example 4.

6. CONCLUSIONS

In this paper, we have proposed a hybrid-damped resolved-acceleration control (HDRAC) to overcome the drawbacks of damped-acceleration resolved-acceleration control (DARAC) and damped-rate resolved-acceleration control (DRRAC). We have shown that, if the DARAC is used, oscillations of the end-effector will occur when the target is outside the workspace and self-motion of the manipulator will appear when the manipulator is at the orientation degeneracy. These phenomena are due to some unnecessary nonzero joint velocities along the degenerated directions. The proposed control scheme removes these unnecessary joint velocities, so that the undesirable phenomena are totally eliminated. The main advantage of the HDRAC is that the control system need not plan the path to avoid the infeasible region, since the controller will automatically command the end-effector to move along the boundary of the workspace with a minimum trajectory error.

The convergent rate of the DRRAC is slower when the end-effector moves to a neighboring region of a singular point, and this region is slightly large.

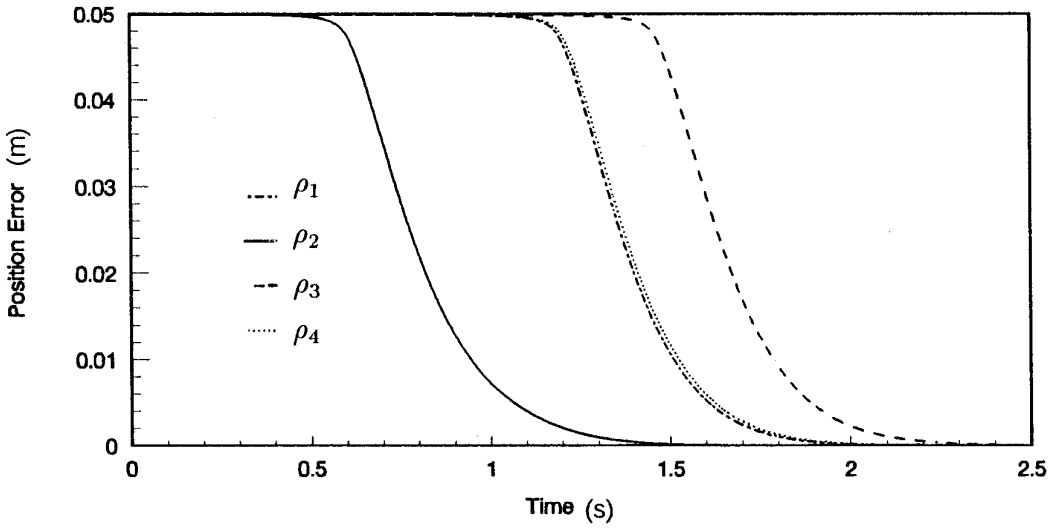

Figure 10. The position errors of ρ_1, ρ_2, ρ_3, and ρ_4 for example 5.

The HDRAC, on the other hand, uses a factor, ρ_r, to reduce the enlarged region to its proper size yet maintain keeping the rate that is similar to that of the DARAC.

This paper has also proven that the proposed control scheme is asymptotically stable. Some simulations are undertaken on the PUMA 560 manipulator. These simulation results show that HDRAC makes the resolved-acceleration control scheme more practical for the industrial manipulator.

In theory, although the end-effector cannot move along the degenerated direction towards the workspace when the manipulator is at the singular point exactly with the DARAC, the DRRAC, or the HDRAC, in practice, it can leave the singular point due to the very small numerical error of the controller computation. But a time delay in this case is unavoidable. Reducing such a time delay will undoubtedly be an interesting subject for future research work.

This article was partially supported by the National Science Council, Taiwan, under Grant NSC83-0422-E-009-066.

REFERENCES

1. J. Y. S. Luh, M. W. Walker, and R. P. Paul, ''Resolved-acceleration control of mechanical manipulators,'' *IEEE Trans. Automatic Control,* AC-25, 195–200, 1980.
2. Y. Nakamura and H. Hanafusa, ''Inverse kinematic solutions with singularity robustness for robot manipulator control,'' *Trans. ASME J. Dynamic Sys., Meas., Contr.,* **108,** 163–171, 1986.
3. C. W. Wampler, ''Manipulator inverse kinematic solution based on vector formulations and damped least-squares methods,'' *IEEE Trans. Sys., Man, Cybern,* **16**(1), 93–101, 1986.
4. C. W. Wampler and L. J. Leifer, ''Applications of damped least-squares methods to resolved-rate and resolved-acceleration control of manipulators,'' *ASME J. Dynamic Sys., Meas., Contr.,* **110,** 31–38, 1988.
5. A. A. Maciejewski and Ch. A. Klein, ''Numerical filtering for the operation of robotic manipulators through kinematically singular configurations,'' *J. Robotic Systems,* **5**(6), 527–552, 1988.
6. S. Chiaverini, ''Estimate of the two smallest singular value of the Jacobian matrix: application to damped least-squares inverse kinematics,'' *J. Robotic Systems,* **10**(8), 991–1008, 1993.
7. M. Kirćanski and M. Dj. Borić, ''Symbolic singular value decomposition for a PUMA robot and its application to a robot operation near singularities,'' *Int. J. Robotics Research,* **12**(5), 460–472, 1993.
8. M. Kirćanski, N. Kirćanski, Dj. Leković, and M. Vukobratović, ''Inverse kinematic problem near singularities for simple manipulators: symbolical damped least-squares solution,'' *Proc. IEEE Int. Conf. Robotics and Automation,* Atlanta, GA, 1993, pp. 974–979.
9. M. Kirćanski, N. Kirćanski, Dj. Leković, and M. Vukobratović, ''An experimental study of resolved acceleration control in singularities: damped least-squares approach,'' *Proc. IEEE Int. Conf. Robotics and Automation,* San Digeo, CA, 1994, pp. 2686–2691.
10. S. K. Lin and S. L. Wu, ''Implementation of the damped resolved acceleration control for a manipulator near singularity,'' *J. Systems Engineering,* **5**(3), 174–191, 1995.
11. L. Kelmar and P. K. Khosla, ''Automatic generation of kinematics for a reconfigurable modular manipulator system,'' *Proc. IEEE Int. Conf. Robotics and Automation,* Philadelphia, PA, 1988, pp. 663–668.
12. A. S. Deo and I. D. Walker, ''Robot subtask performance with singularity robustness using optimal damped least-squares,'' *Proc. IEEE Int. Conf. Robotics and Automation,* Nice, France, 1992, pp. 434–441.
13. A. S. Deo and I. D. Walker, ''Adaptive non-linear least squares for inverse kinematics,'' *Proc. IEEE Int. Conf. Robotics and Automation,* Atlanta, GA, 1993, pp. 186–193.
14. R. V. Mayorga, N. Milano, and A. K. C. Wong, ''A damped least-squares solution to manipulator inverse kinematics and singularities prevention,'' *Int. J. Robotics and Automation,* **7**(4), 171–178, 1992.
15. R. V. Mayorga, A. K. C. Wong, and N. Milano, ''A fast procedure for manipulator inverse kinematics evaluation and pseudoinverse robustness,'' *IEEE Trans. Sys., Man, Cybern,* **22**(4), 790–798, 1992.
16. A. A. Maciejewski and Ch. A. Klein, ''The singular value decomposition: computation and applications to robotics,'' *Int. J. Robotics Research,* **8**(6), 63–79, 1989.
17. S. Chiaverini, O. Egeland, and K. Kanestrom, ''Achieving user-defined accuracy with damped least-squares inverse kinemat,'' *Proc., 1991 Fifth Int. Conf. Advanced Robotics,* Pisa, Italy, vol. 2, 1991, pp. 672–677.
18. S. L. Wu and S. K. Lin, ''Damped-rate resolved-acceleration control for manipulator,'' *Proc. of 13th IFAC World Congress,* San Francisco, CA, vol. A, 1996, pp. 349–354.
19. T. Yoshikawa, ''Manipulability of robotic mechanisms,'' *Int. J. Robotics Research,* **4**(2), 3–9, 1985.
20. S. K. Lin, ''Robot control in Cartesian space,'' in *Progress in Robotics and Intelligent Systems,* Vol. 3, G. W. Zobrist and C. Y. Ho Eds., Ablex, New Jersey 1995, pp. 85–124.
21. C. H. Lawson and R. J. Hanson, *Solving Least Squares Problems,* Prentice-Hall, Englewood Cliffs, NJ, 1974.
22. B. Noble and J. W. Daniel, *Applied Linear Algebra,* 3rd ed., Prentice-Hall, Englewood Cliffs, NJ, 1988.
23. S. K. Lin, ''Microprocessor implementation of the inverse dynamic system for industrial robot control,'' *Proc. of 10th IFAC World Congress on Automatic Control,* vol. 4, 1987, pp. 332–339.
24. S. K. Lin, *Aufbau von Modellen zur Largeregelung von Industrierobotern,* Carl Hanser Verlag, Munich, Germany 1989.